Volume 18
Number 1
January 1979

Inorganic Chemistry

Contribution from the Department of Chemical Engineering, University of Waterloo, Waterloo, Ontario, Canada

μ_3-Oxo-triruthenium Acetate Cluster Complexes as Catalysts for Olefin Hydrogenation

S. A. FOUDA and G. L. REMPEL*

Received July 13, 1978

μ_3-Oxo-triruthenium(III) acetate, $[Ru_3O(OCOCH_3)_6(H_2O)_3][OCOCH_3]$, when treated with H_2 in dimethylformamide was found to be effective in providing novel triruthenium acetate cluster complexes which were active for the quantitative hydrogenation of a variety of olefinic and acetylenic compounds in dimethylformamide at 80 °C. Initially, the hydrogenation of the unsaturated substrate was catalyzed by the monohydridic triruthenium cluster complex $[HRu_3O(OCOCH_3)_5(DMF)_3][OCOCH_3]$ which was also found to catalyze the isomerization of terminal olefins in the absence of hydrogen. In the case of terminal and internal straight chain olefins, this monohydride triruthenium cluster was found to undergo a facile intramolecular reduction to form $[Ru_3O(OCOCH_3)_4(DMF)_n][OCOCH_3]$. This cluster complex served as the catalyst for the major part of the olefin hydrogenation. The results of a detailed kinetic study are reported, and a plausible mechanism is presented for the hydrogenation of dec-1-ene in dimethylformamide. A very important and significant finding of this study is that only one ruthenium center of the cluster complex ion, $[Ru_3O(OCOCH_3)_4(DMF)_n]^+$, is active in coordinating both the hydrogen and the olefin molecule and in transferring the hydrogen to the olefin. Although the other two ruthenium centers of the cluster also possess coordinative unsaturation, they function merely as metal entities present in a polydentate ligand. These metal entities do not appear to become involved in coordination to the reacting molecules.

Introduction

Mechanistic studies on the presently little explored metal cluster complexes appear to be particularly important with respect to gaining further insight into catalytic phenomena.[1] The results of several catalytic studies indicate that often complexes emerge as dimers, trimers, etc., in the catalytic reaction. However, a dimeric or trimeric structure for the catalytic complex in itself does not answer the question as to whether more than one metal atom of the cluster complex participates in the catalytic process or whether one metal atom functions as the active center and the other adjacent metal centers function as ligands in relation to the active center. Thus, kinetic and mechanistic studies with polymetallic complexes under homogeneous conditions may provide further insight into this question as well as important information about the mechanistic features of their heterogeneous counterparts.

Although numerous reports on the use of ruthenium complexes as catalysts for homogeneous hydrogenation have been published,[2,3] little information on the activity and mechanistic implications of complexes having more than one ruthenium center is available.[3,4] A considerable amount of work has been carried out on the redox and substitution reactions of oxotriruthenium cluster complexes such as $[Ru_3O(OCOCH_3)_6(H_2O)_3][OCOCH_3]$;[5] however, no report of their direct use as hydrogenation catalysts has been made. Wilkinson and co-workers[6] have prepared a number of complexes from the oxotriruthenium cluster which do exhibit catalytic activity, but all these active catalytic species no longer contain the triruthenium cluster. In this paper, we report on the detailed kinetics and mechanism of the homogeneously catalyzed hydrogenation of olefins by oxotriruthenium acetate complexes obtained via hydrogen reduction of $[Ru_3O(OCOCH_3)_6(H_2O)_3][OCOCH_3]$ in dimethylformamide.

Experimental Section

$[Ru_3O(OCOCH_3)_6(H_2O)_3][OCOCH_3]$ was prepared from commercially available "ruthenium trichloride trihydrate" (Engelhard Industries Ltd.), according to a procedure based on that given by Wilkinson and co-workers.[7,8] Four grams of "$RuCl_3 \cdot 3H_2O$" together with 7 g of $NaOCOCH_3 \cdot 3H_2O$ was dissolved in a mixture of 75 mL of glacial acetic acid and 75 mL of ethanol. The solution was refluxed under nitrogen for approximately 2 h, during which time the initial reddish brown color of the solution changed to dark green. The solution was cooled to −30 °C and decanted to separate precipitated sodium chloride and sodium acetate. The decanted solution was then filtered and the filtrate was taken to dryness. The solid thus obtained is the crude oxotriruthenium(III) acetate complex. The resulting crude acetate complex was dissolved in a minimum amount of ethanol and cooled to −30 °C overnight. Sodium acetate and sodium chloride were precipitated and separated by filtration. The filtrate was taken to dryness and the solid was washed with benzene to remove excess acetic acid. Several extractions with ethanol (ca. four to six) were performed until no more precipitate was apparent on filtration. This final filtrate was taken to dryness and after a final benzene wash, the product was dried in vacuo over sodium hydroxide pellets at 60 °C overnight; yield 3.2 g (80% on the basis of Ru content of "$RuCl_3 \cdot 3H_2O$"). Anal. Calcd for $C_{14}H_{27}O_{18}Ru_3$: C, 21.30; H, 3.44. Found: C, 20.97; H, 3.36. The electronic spectra and infrared spectra agreed with that reported previously.[7]

Reagent grade chemicals and solvents were used throughout. Dimethylformamide was purified by storing over CaH_2 under N_2 for at least 40 h followed by distillation under reduced pressure; the constant-boiling fraction was collected onto Linde 4A molecular sieve and stored under Linde ultrahigh-purity nitrogen.

Dec-1-ene, obtained from Aldrich, was freed from peroxides by treatment with ferrous sulfate. When the potassium thiocyanate–ferrous sulfate test was negative, the dec-1-ene was distilled from sodium under nitrogen. The distillate was stored over molecular sieve under nitrogen and protected from light. Linde ultrahigh-purity H_2 and Matheson CP grade D_2 were passed through an Engelhard deoxo purifier before admission to the kinetic apparatus.

0020-1669/79/1318-0001$01.00/0

Table I. Relative Rates of Hydrogenation of Substrates Using Oxotriruthenium Acetate in DMF at 80 °C ($[Ru_3]$ = 7.68 mM; [substrate] = 0.10 M; $[H_2]$ = 2.75 mM)

substrate	rel max rate
dec-1-ene	1.00
oct-1-ene	1.07[a]
oct-2-ene	1.07[a]
cyclooctene	1.43[a]
oct-1-ene	2.13[b]
oct-2-ene	2.99[b]
cyclooctene	4.80[b]
hex-1-en-3-ol	0.30[a]
cyclohex-2-en-1-ol	1.10[a]
cyclohex-3-en-1-ol	0.26[a]
hex-1-yne	0.32[a]
oct-1-yn-3-ol	0.17[a]
trans-stilbene	0.51
maleic acid	0.44[c]
maleic anhydride	0.35[c]
diethyl maleate	0.24
pentan-3-one	very slow[a]
C_2H_4	3.73×10^{-6} M s^{-1} [d]
O_2	0.73×10^{-6} M s^{-1} [e]

[a] Substrate used as received from manufacturer. [b] Substrate purified as for dec-1-ene (see Experimental Section). [c] Recrystallized. [d] $P_{C_2H_4}$ = 380 mmHg; P_{H_2} = 375 mmHg; first stage Ru_3 product prepared prior to C_2H_4 admission. [e] P_{O_2} = 320 mmHg; P_{H_2} = 435 mmHg.

UV–visible spectra were recorded on a Beckman DK2. GLC analysis was carried out using a Hewlett-Packard F&M Scientific 700 laboratory chromatograph. A 12-ft column of Union Carbide 10% UC-W 98 at 90 °C was used for analysis of isomerized and hydrogenated olefins. Emf measurements as well as potentiometric titrations were carried out using a Radiometer pH Meter 26 with glass and calomel electrodes. A Yellow Springs Model YS1-31 conductivity bridge was used for conductivity measurements. NMR spectra were obtained on a Varian HR 100 and a Bruker Spectrospin 60-MHz instrument.

Air-sensitive compounds and solutions were handled inside a Dri-Lab glovebox equipped with a Dri Train, both obtained from Vacuum Atmospheres Co.

Chemical analyses were obtained from Galbraith Laboratories, Knoxville, Tenn.

Kinetic measurements were made by following the consumption of hydrogen at constant pressure using the apparatus and procedure described earlier.[9] The solubility of H_2 in dimethylformamide was determined as 2.75×10^{-3} M at a total pressure of 760 mmHg and 80 °C, Henry's law being obeyed at least up to 1 atm.

Results

Solutions of $[Ru_3O(OCOCH_3)_6(H_2O)_3][OCOCH_3]$ in DMF were found to hydrogenate terminal, internal, and cyclic monoenes homogeneously at 80 °C under 1 atm of hydrogen. Comparative rates under standard conditions are provided in Table I. From these results the following reactivity order is apparent: cyclic alkene > internal alkene > terminal alkene > terminal alkyne.

Representative hydrogen consumption plots for the hydrogenation of dec-1-ene are shown in Figure 1. The overall reaction exhibits an autocatalytic nature. The length of the initial induction period observed was found to depend upon the initial ruthenium concentration as shown in Figure 2. Furthermore, there is a noticeable leveling of the consumption rate before the ultimate maximum rate region is achieved. The uptake of hydrogen then terminates in an apparent first-order fashion.

Stoichiometry of Hydrogenation. The total hydrogen consumption leveled off at an amount close to that required for complete hydrogenation of the olefinic substrate and 1 mol of hydrogen/mol of oxotriruthenium(III) acetate. Analyses of the final product solutions by GLC indicated complete conversion of the olefin to the paraffin.

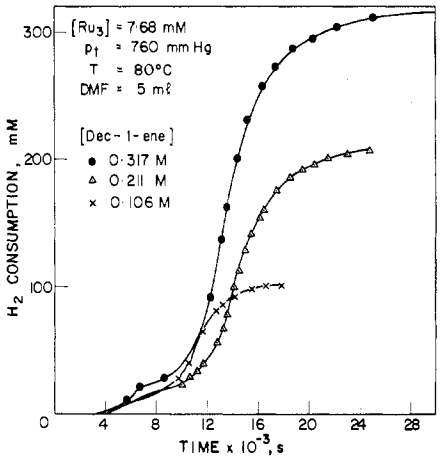

Figure 1. Representative hydrogen consumption plots for the hydrogenation of dec-1-ene using oxotriruthenium(III) acetate.

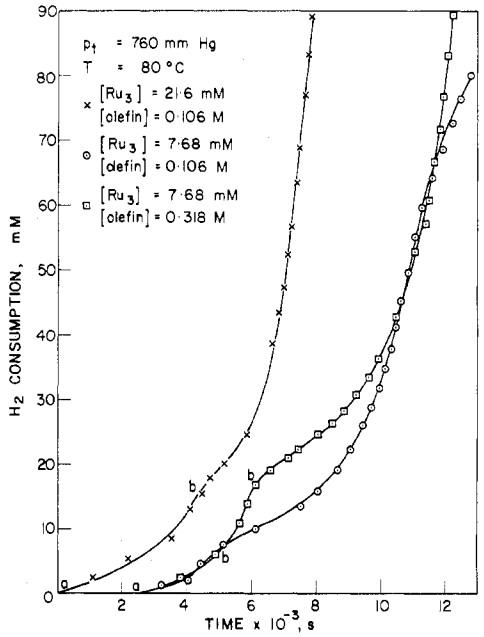

Figure 2. Representative hydrogen consumption plots for the hydrogenation of dec-1-ene using oxotriruthenium(III) acetate.

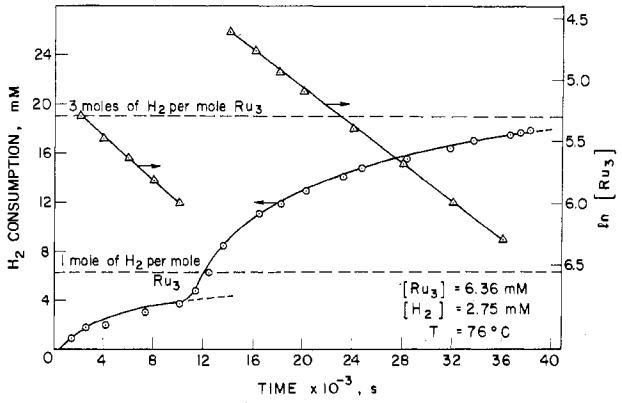

Figure 3. Representative hydrogen consumption plot for the H_2 reduction of oxotriruthenium(III) acetate.

In the absence of olefinic substrate, oxotriruthenium(III) acetate was found to consume 1 mol of hydrogen[10] in a time interval which was very close to the length of the initial induction period occurring before achievement of the maximum rate region of the olefin hydrogenation experiments (compare Figures 2 and 3). After termination of olefin hydrogenation

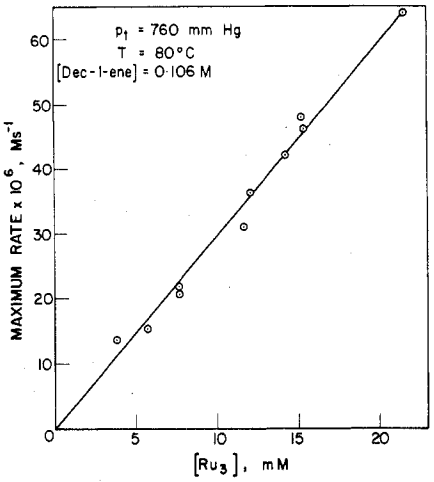

Figure 4. Hydrogenation of dec-1-ene using oxotriruthenium(III) acetate. Effect of $[Ru_3]$ on maximum hydrogenation rate.

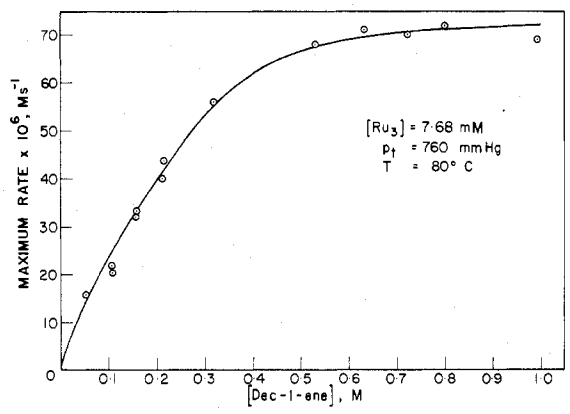

Figure 5. Hydrogenation of dec-1-ene using oxotriruthenium(III) acetate. Effect of [dec-1-ene] on maximum hydrogenation rate.

or in cases where no olefin was used, a further relatively slow reaction, of the 1:1 H_2–oxotriruthenium(III) acetate product, with hydrogen occurred[10] as shown in Figure 3.

Kinetics of Olefin Hydrogenation. The kinetic data for the olefin hydrogenation reaction were analyzed by determining the slope of the linear portion of the maximum rate region. The uptake plot showed first-order behavior near the end of the reaction according to the equation

$$-d[\text{olefin}]/dt = k'[\text{olefin}] \qquad (1)$$

Good linear plots of ln [olefin] vs. time provided values of k'. The effect of reagent concentration variables on k' values was consistent with the effect observed on the maximum rate values. Thus the slopes of the plots at the maximum rate region were used for analyzing the data.

A first-order dependence of the hydrogenation rate on $[Ru_3]$ is apparent from a plot of the maximum rate vs. $[Ru_3]$ as shown in Figure 4. Figure 5 shows that the rate of hydrogenation is first order in [dec-1-ene] at low[dec-1-ene] and that the rate tends to a zero-order dependence in [dec-1-ene] at higher [dec-1-ene]. A plot of the maximum rate of hydrogenation as a function of $[H_2]$, as shown in Figure 6, suggests a first-order dependence on $[H_2]$ over this concentration range.

A number of experiments were conducted in which lithium acetate was added to the reaction solution over the concentration range of 0–3 mM (3 mM being the maximum solubility obtainable in DMF). The effect of added acetate was studied at two different [dec-1-ene], namely, 0.156 and 0.739 M. These two [dec-1-ene] represent respectively regions where a first-order and zero-order rate dependence on [dec-1-ene]

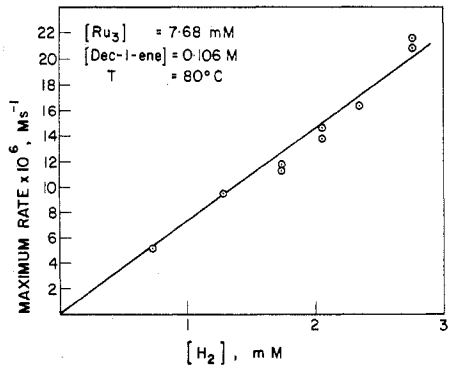

Figure 6. Hydrogenation of dec-1-ene using oxotriruthenium(III) acetate. Effect of $[H_2]$ on maximum hydrogenation rate.

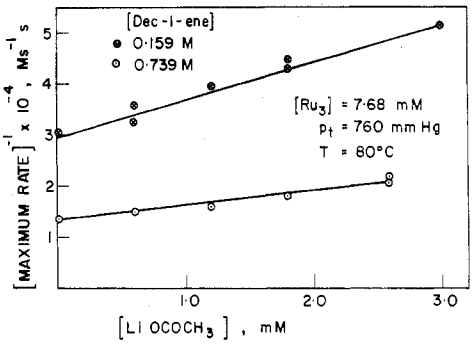

Figure 7. Hydrogenation of dec-1-ene using oxotriruthenium(III) acetate. Effect of added $[LiOCOCH_3]$ on maximum hydrogenation rate.

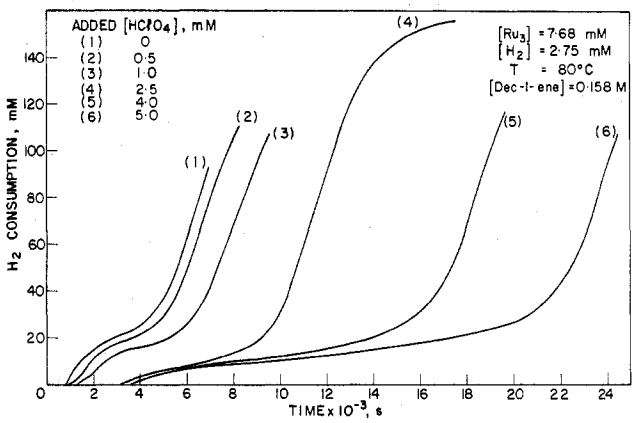

Figure 8. Hydrogenation of dec-1-ene using oxotriruthenium(III) acetate. Effect of added $[HClO_4]$ on hydrogenation reaction.

were found. Good linear plots, as shown in Figure 7, were obtained when the inverse of the maximum rate was plotted against the added $[LiOCOCH_3]$. Since the highest $[LiOCOCH_3]$ was less than 50% of the $[Ru_3]$ and since $[LiClO_4]$ as high as 0.01 M had virtually no effect on the reaction rate, no compensation for the ionic strength was made. Also, the addition of small amounts of water to the extent of that present on addition of the $LiOCOCH_3$ did not influence the rate of hydrogenation.

A series of experiments were carried out in which given amounts of perchloric acid were added to the initial reaction solution in an attempt to study the effect of proton concentration on the rate of the hydrogenation reaction. When the range of $[HClO_4]$ used for this purpose was 0–5 mM with $[Ru_3]$ = 7.68 mM, an increase in the initial induction period of the hydrogen consumption plot was observed as shown in Figure 8. Once the maximum rate region was achieved, a small random effect of the initial added acid concentration

Table II. Hydrogenation of Dec-1-ene Using μ_3-Oxo-triruthenium Acetate and Effect of Added Acid on the Rate of Hydrogenation

$10^3[HClO_4]$, M	max rate $\times 10^6$, M s^{-1}	% dev from the av
[Dec-1-ene] = 0.158 M; $[Ru_3] = 7.68 \times 10^{-3}$ M; $[H_2] = 2.75 \times 10^{-3}$ M; $T = 80$ °C		
0.0	32.4	4.14
0.5	29.0[a]	−6.79
1.0	28.0[a]	−10.00
2.5	33.0[a]	6.07
4.0	32.0[a]	2.85
5.0	33.0[a]	6.07
10.0	32.0[b]	2.85
17.6	30.0[b]	−5.18
[Dec-1-ene] = 0.739 M; $[Ru_3] = 7.68 \times 10^{-3}$ M; $[H_2] = 2.75 \times 10^{-3}$ M; $T = 80$ °C		
0.0	64	−9.2
0.0	70	−0.7
5.0	70[b]	−0.7
10.0	78[b]	10.6

[a] Acid added initially in the reaction mixture. [b] Acid added at a point in the maximum rate region.

on the maximum rate resulted as shown in Table II. This small random effect was within the reproducibility of the experimental rate measurements (i.e., ±10%). Further experiments on the study of the effect of added protons on the reaction rate were carried out, whereby the reaction was stopped in the maximum rate region and excess amounts of acid (over $[Ru_3]$) were added. Table II shows that essentially no effect of the added acid (as high as 17.6 mM) on the maximum rate was observed at two different [dec-1-ene], namely 0.158 M (first-order region of olefin dependence) and 0.739 M (zero-order region of olefin dependence).

Discussion

Nature of the Hydrogenation Catalyst. Studies in the absence of olefinic substrate indicate that oxotriruthenium(III) acetate is capable of activating hydrogen to form initially a monohydride triruthenium complex $[HRu_3O(OCOCH_3)_5(DMF)_3][OCOCH_3]$ which decays to form $[Ru_3O(OCOCH_3)_4(DMF)_n][OCOCH_3]$.[10] In the absence of a reducible substrate, this species undergoes further reduction by hydrogen as shown in Figure 3. In the presence of substrate, however, it seems reasonable to expect that the monohydride complex and perhaps its decay product are potential catalysts for olefin hydrogenation.

Thus, the hydrogenation cycle could be written as shown in eq 2–4 if the monohydride triruthenium complex were the

$$[Ru_3O(OCOCH_3)_6][OCOCH_3] + H_2 \underset{k_{-1}}{\overset{k_1}{\rightleftharpoons}} \underset{\text{B}}{[HRu_3O(OCOCH_3)_5][OCOCH_3]} + HOCOCH_3 \quad (2)$$

terminal ligands omitted

$$B + \text{olefin} \overset{K}{\rightleftharpoons} B(\text{olefin}) \rightarrow B'(\text{alkyl}) \quad (3)$$

$$B'(\text{alkyl}) + H_2 \xrightarrow{k} B + \text{paraffin} \quad (4)$$

active catalyst. The mechanistic scheme shown in eq 2–4 predicts that the rate of hydrogen uptake increases as more of species B is formed and a maximum rate is achieved when all the ruthenium complex is in the form of B. Although the hydrogen consumption plots show an autocatalytic nature, the increase in the rate of uptake with time is not consistently observed along the initial part of the reaction. Figure 2 shows a leveling in the rate of uptake which follows an autocatalytic portion ab and precedes the attainment of the maximum rate region. This strongly suggests that two different reactive

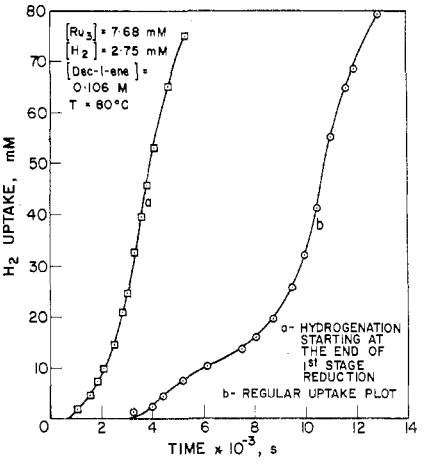

Figure 9. Hydrogenation of dec-1-ene using oxotriruthenium(III) acetate. Comparison of reaction profile of hydrogenation starting with $[HRu_3O(OCOCH_3)_5(DMF)_3][OCOCH_3]$ (plot a) with that obtained when starting with $[Ru_3O(OCOCH_3)_6(DMF)_3][OCOCH_3]$ (plot b).

intermediates may be involved in the catalytic reaction. As the triruthenium monohydride complex catalyzes the hydrogenation, probably via a mechanism such as that shown in eq 2–4 above, a concurrent process that does not consume hydrogen takes place and results in the formation of a more reactive intermediate. Reactions of oxotriruthenium(III) acetate with hydrogen in the absence of olefin[10] leads to the conclusion that this concurrent process is the decay of the triruthenium monohydride complex to a triruthenium species of a lower average oxidation state as depicted in reaction 5.

$$\underset{\text{B}}{[HRu_3O(OCOCH_3)_5][OCOCH_3]} \rightarrow \underset{\text{C}}{[Ru_3O(OCOCH_3)_4][OCOCH_3]} + HOCOCH_3 \quad (5)$$

DMF ligands omitted

When the reaction of oxotriruthenium(III) acetate with hydrogen was stopped at the end of the first stage, i.e., when species B was formed, the addition of protons under oxygen-free conditions caused a fast back-reaction to give the starting oxotriruthenium(III) acetate as indicated by the visible absorption spectra. However, when the hydrogenation reaction was stopped in the maximum rate region, i.e., when species C was presumably fully formed, the addition of protons under oxygen-free conditions did not change the spectra of the solution. When a solution of either B or C was exposed to air, oxotriruthenium(III) acetate was rapidly restored. This suggests that the trimeric structure of the initial oxotriruthenium(III) acetate is preserved in species B and C. Titration of a DMF solution of B, formed from H_2 reduction of oxotriruthenium(III) acetate, with sodium methoxide indicated 1 mol of acetic acid/mol of Ru_3, whereas such a titration for a DMF solution of species C indicated 2 mol of acetic acid/mol of Ru_3. This is in agreement with the formation of species B and C via eq 2 and 5, respectively.

From the above observations, it can be concluded that although the species B is not inactive toward hydrogenation (i.e., Figure 2), the reactive species that catalyzes the hydrogenation in the maximum rate region is species C. Plot a in Figure 9 shows a hydrogen consumption plot for olefin hydrogenation by a solution of oxotriruthenium(III) acetate pretreated with H_2 to form species B. Plot a exhibits a normal autocatalytic nature; the time consumed before the gas uptake was measurable is due to the attainment of vapor–liquid equilibrium, as well as the intramolecular reduction of species B to species C according to eq 5. When the conductivity of the reaction solution in the maximum rate region of hydro-

genation of decene was measured, the molar conductance of species C in DMF was found to have a value of 127 Ω^{-1} cm^2 mol^{-1} at [Ru_3] = 0.1 mM and 30 °C. This indicates that the acetate resulting in the acetic acid produced in eq 5 arises from one of the acetate bridges of species B. (The molar conductance of species B in DMF was measured as 57 Ω^{-1} cm^2 mol^{-1} and that of the initial oxotriruthenium(III) acetate in DMF as 44 Ω^{-1} cm^2 mol^{-1}, when [Ru_3] = 0.1 mM and T = 30 °C.)

Hydrogenation Mechanism. The above considerations suggest that the catalytic hydrogenation of dec-1-ene takes place via two different reactive intermediates, namely, a monohydride triruthenium complex, $[HRu_3O(OCOCH_3)_5(DMF)_3][OCOCH_3]$, and its intramolecular reduction product $[Ru_3O(OCOCH_3)_4(DMF)_n][OCOCH_3]$ in which each ruthenium center has an average oxidation state of $^7/_3$.[10] The hydrogenation via the monohydride complex is predominant in the initial part of the reaction and is more pronounced when high olefin concentrations are used (see Figure 1). The hydrogenation via $[Ru_3O(OCOCH_3)_4(DMF)_n][OCOCH_3]$ contributes the most in the overall hydrogenation process and takes place exclusively in the maximum rate region.

Hydrogenation via $[HRu_3O(OCOCH_3)_5(DMF)_3][OCOCH_3]$. The mechanism of the dec-1-ene hydrogenation reaction that takes place initially could be outlined in a scheme as given by eq 2–4 above. In this reaction scheme the formation of the monohydride has been established in the absence of olefin.[10] In the second step, it is assumed that π-complex formation occurs between the alkene and the hydridic species followed by an insertion of the coordinated alkene into the Ru–H bond to form an alkyl complex. This step seems very feasible since the triruthenium monohydride species B resulting from reaction 2 was found to isomerize dec-1-ene even in the absence of hydrogen. The rate-determining step (i.e., eq 4) proposed in the scheme involves the interaction of a hydrogen molecule with the σ-alkyl complex which results in the formation of the saturated product and regeneration of species B. This mechanism is analogous to that postulated for the catalytic hydrogenation of olefins using the monomeric ruthenium catalyst $RuHCl(P(C_6H_5)_3)_3$.[11] Since no kinetic data can easily be extracted for the hydrogenation that occurs in the initial region of the present system, it is not clear whether reaction 3 is a rapidly established equilibrium or a reversible rate-determining step. The olefin could coordinate to the same ruthenium center where the hydride is bound or for steric preference it could possibly coordinate to an adjacent ruthenium atom which had lost one acetate bridge in the first step (reaction 2). Such an intermediate is suggested in the case of olefin-catalyzed hydrogenation via $Rh_2(OCOCH_3)_4$.[12] Should further hydrogen interaction of species B take place prior to olefin interaction, no site would be readily available for coordination of the olefin. Furthermore, the reaction of oxotriruthenium(III) acetate with hydrogen in the absence of a substrate (see Figure 3) was shown to exhibit a leveling in the hydrogen consumption after the formation of species B and little additional uptake of hydrogen occurs until the intramolecular reduction product (i.e., species C in reaction 5) is appreciably formed.

Hydrogenation via $[Ru_3O(OCOCH_3)_4(DMF)_n][OCOCH_3]$. The strict first-order dependence of the rate of reaction on [Ru_3] indicates that each trimeric entity is involved in one catalytic cycle; this does not rule out the possibility of two adjacent ruthenium atoms of the trimetallic species being involved in the hydrogenation cycle (i.e., subsequent olefin activation at an adjacent site). It does, however, rule out the homolytic splitting of hydrogen as the mode of activation.

To study the effect of added protons on the rate of the reaction, a series of experiments were carried out where various

Scheme I

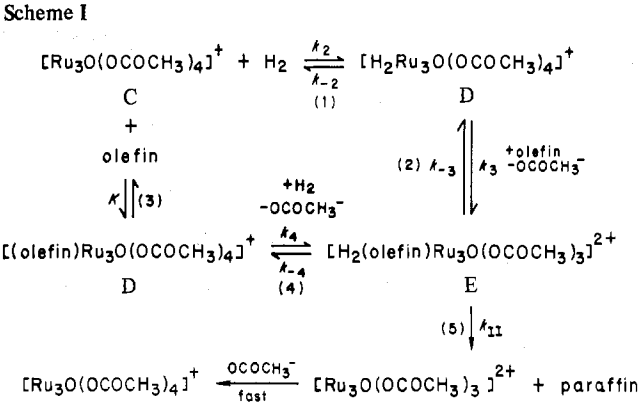

amounts of perchloric acid were initially added to the reaction solution ([$HClO_4$]:[Ru_3] < 1:1). Figure 8 shows that the presence of protons at the start of the overall reaction causes longer periods of time before the achievement of the maximum rate. Once the maximum rate was achieved, no significant change on the value of the maximum rate was observed. Emf measurements of the solution at the maximum rate region indicated that the free protons initially added were consumed during these long induction periods. This is undoubtedly due to the formation of the perchlorate salt of the oxotriruthenium acetate complex as shown in eq 6.

$$[Ru_3O(OCOCH_3)_6][OCOCH_3] + HClO_4 \rightarrow [Ru_3O(OCOCH_3)_6][ClO_4] + HOCOCH_3 \quad (6)$$

DMF ligands omitted

Reaction 6 also seems to occur in the preparation of the analogous acetato(oxo)trirhodium perchlorate from the acetato(oxo)trirhodium acetate.[13] When the concentration of perchloric acid was kept lower than [Ru_3], the free protons only enhance the reverse of reaction 2, preventing further reaction from taking place, until the process shown in reaction 6 causes the removal of most of the free protons from the solution. It is thus obvious that a meaningful proton dependence could only be obtained if the amount of added acid exceeds [Ru_3]. This, however, resulted in exceedingly long waiting periods before the maximum rate region was achieved. The proton dependence was consequently studied by carrying out the hydrogenation experiment and stopping the reaction in the maximum rate region. At this point the reaction solution was frozen and the perchloric acid was added (in higher concentration than [Ru_3]) under oxygen-free conditions. The rate of the reaction was then measured with the assurance that the free protons exist per se in solution. When the above mentioned procedure was used, no significant effect of added protons on the rate of the reaction was observed as shown in Table II. This is in direct contrast to the inhibition by added protons found when no substrate was present.[10] On the basis of this result, the activation of hydrogen for the olefin hydrogenation is considered to be via a dihydride formation at a ruthenium center of the intramolecular reduction product (i.e., species C in reaction 5).

Scheme I incorporates the two general paths that have been recognized for transfer of the hydrogen molecule to an olefin via a homogeneous hydrogenation catalyst. Whether the hydrogenation process occurs predominantly via the unsaturate path or via the hydride path, step 4 or 2, respectively, must be invoked in order to account for the observed inverse dependence of added acetate on the rate of hydrogenation. Both the unsaturate and hydride paths result in the same reactive intermediate E.

Unsaturate Path. Steps 3, 4, and 5 of Scheme I represent the unsaturate path whereby a preequilibrium between the triruthenium species C and the olefinic substrate occurs prior

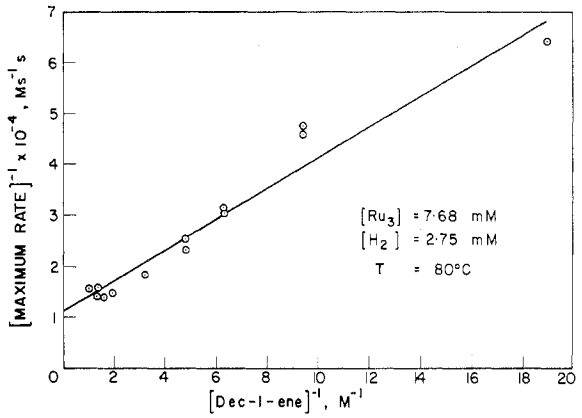

Figure 10. Hydrogenation of dec-1-ene using oxotriruthenium(III) acetate: (maximum rate)$^{-1}$ vs. [dec-1-ene]$^{-1}$.

to interaction with hydrogen. If the hydrogenation were to take place primarily via this path, a rate law of the form shown in eq 7 would be obtained, provided a steady-state concentration for species E is assumed. This rate law when written in inverse form is as shown in eq 8. Equation 8 predicts that

$$\frac{-d[H_2]}{dt} = \frac{Kk_4k_{II}[Ru_3]_T[olefin][H_2]}{(1 + K[olefin])(k_{-4}[OCOCH_3^-] + k_{II})} \quad (7)$$

subscript T refers to total concentration

$$\left[\frac{-d[H_2]}{dt}\right]^{-1} = \frac{k_{-4}[OCOCH_3^-] + k_{II}}{Kk_4k_{II}[Ru_3]_T[H_2]}\frac{1}{[olefin]} + \frac{k_{-4}[OCOCH_3^-] + k_{II}}{k_4k_{II}[Ru_3]_T[H_2]} \quad (8)$$

a plot of $1/[-d[H_2]/dt]$ vs. $1/[olefin]$ should be linear. Figure 10 shows that on treating the observed kinetic data via such a plot a fairly linear[18] line having a slope of 3080 ± 213 s^{-1} and an intercept of $(1.13 \times 10^4) \pm (0.16 \times 10^4)$ M s^{-1} is obtained. The ratio of the intercept to the slope of this line affords a value for the equilibrium constant K, as can easily be seen from eq 8. The estimated value of K, as obtained from this ratio, is 3.67 ± 0.7 M^{-1}.

Spectral examination of a DMF solution of species C (i.e., [decene]:[C] = ca. 100:1) indicated no detectable change in the absorption spectra, in the region of 750–270 nm which could be attributed to complex formation. If K were to have a value of ca. 2–4 M^{-1}, some change in the electronic absorption spectra would be expected.[14] Consequently, it is concluded that the unsaturate path, if it does occur at all, is not the predominant path for the hydrogenation.

Hydride Path. In Scheme I steps 1, 2, and 5 represent the hydride path. Step 1 is proposed as a reversible rate-determining step rather than a rapidly established equilibrium, since no evidence for the latter was apparent. Furthermore, when the hydride path is the predominant hydrogenation path, consideration of step 1 as a rapid equilibrium does not lead to a rate law having an inverse olefin dependence at high [olefin]. The observed kinetic data are in accord with step 1 as a reversible rate-determining step. If a steady-state concentration for species D and E is assumed, the mechanism outlined by steps 1, 2, and 5 gives rise to the rate law shown in eq 9. Equation 9 can alternatively be written in inverse form as shown in eq 10. At high [olefin], the rate is independent of [olefin] at no added acetate; thus, the rate law applicable is as shown in eq 11. At low [olefin] the rate is first order in [olefin] and the rate law given by eq 9 can be written as shown in eq 12. Equation 12 when expressed in inverse form is given by eq 13. According to eq 10 a plot of $[-d[H_2]/dt]^{-1}$ vs. $[olefin]^{-1}$ should be linear with an intercept of $(k_2[Ru_3]_T[H_2])^{-1}$. Figure 10 shows that a straight line is obtained on plotting the inverse of the maximum rate against the inverse of the olefin concentration. From the intercept of Figure 10 a value of k_2 is estimated as 4.2 M^{-1} s^{-1}. Application of eq 11 to experiments carried out at high olefin concentration (i.e., zero-order region of the olefin dependence) provides an average value for k_2 of 3.23 M^{-1} s^{-1}. In view of the difficulty in determining accurate values of intercepts from inverse plots, the two values for k_2 are in fair agreement.

$$\frac{-d[H_2]}{dt} = \frac{k_2k_3k_{II}[Ru_3]_T[H_2][olefin]}{k_{-2}k_{-3}[OCOCH_3^-] + k_3k_{II}[olefin] + k_{-2}k_{II}} \quad (9)$$

$$\left[\frac{-d[H_2]}{dt}\right]^{-1} = \left[\frac{k_2k_{-3}[OCOCH_3^-] + k_{-2}k_{II}}{k_2k_3k_{II}}\right]\left[\frac{1}{[Ru_3]_T[H_2][olefin]}\right] + \frac{1}{k_2[Ru_3]_T[H_2]} \quad (10)$$

$$-d[H_2]/dt = k_2[Ru_3]_T[H_2] \quad (11)$$

$$\frac{-d[H_2]}{dt} = \frac{k_2k_3k_{II}[Ru_3]_T[H_2][olefin]}{k_{-2}k_{-3}[OCOCH_3^-] + k_{-2}k_{II}} \quad (12)$$

$$\left[\frac{-d[H_2]}{dt}\right]^{-1} = \frac{k_{-2}k_{-3}[OCOCH_3^-]}{k_2k_3k_{II}[Ru_3]_T[H_2][olefin]} + \frac{k_{-2}}{k_2k_3[Ru_3]_T[H_2][olefin]} \quad (13)$$

For experiments carried out at low olefin concentration a plot of $[-d[H_2]/dt]^{-1}$ vs. $[OCOCH_3^-]$ is linear as shown in Figure 7. Equation 13 predicts that the ratio of the intercept to the slope of such a line is equal to k_{II}/k_{-3}. The ratio obtained for k_{II}/k_{-3} from this line (see Figure 7, line for [dec-1-ene] = 0.158 M) has a value of 230.7 M^{-2} s. When the average value of k_2 obtained above (i.e., ca. 3.75 M^{-1} s^{-1}) is considered together with the value of the intercept of Figure 7, the ratio of k_{-2}/k_3 is estimated to be 0.38 M.

The above discussion on the unsaturate and hydride paths indicates that although the experimental rate law can be obtained when either path is predominating, the hydride path is favored. This conclusion was arrived at primarily on the basis of the results obtained for the hydrogen reduction of $[Ru_3O(OCOCH_3)_6(DMF)_3][OCOCH_3]$ in the absence of a substrate and that complex formation between the reduced species C (see Scheme I) and dec-1-ene was not observed.

At high olefin concentration the rate law for the hydrogenation reaction was shown to have the form of eq 11. Consequently, the effect of temperature on the reaction at high olefin concentration provides the activation parameters associated with the rate process defined by k_2 (i.e., formation of the dihydride species D in Scheme I). The activation energy associated with the k_2 step was evaluated from the Arrhenius plot shown in Figure 11. The value obtained for the activation energy was 19.5 ± 0.6 kcal/mol. At 80 °C the enthalpy of activation for the k_2 step is estimated to be 18.8 ± 0.6 kcal/mol and the entropy of activation is calculated as −3.2 ± 1.7 eu.

At low olefin concentration the overall rate law is given by eq 12. The activation parameters obtained at low olefin concentration are associated with a composite rate constant as defined by eq 12. A good Arrhenius plot as shown in Figure 11 is obtained for the temperature rate data obtained at low olefin concentration, and an apparent activation energy of 10.2 ± 0.8 kcal/mol is obtained from this plot.

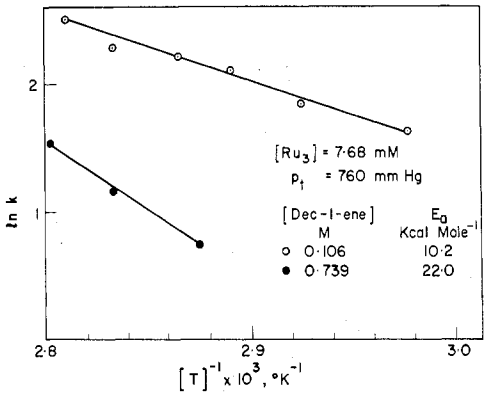

Figure 11. Hydrogenation of dec-1-ene using oxotriruthenium(III) acetate: Arrhenius plots.

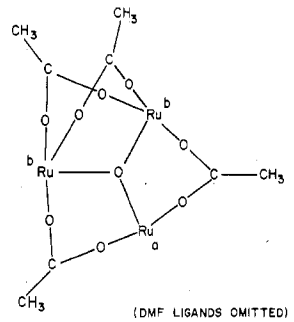

Figure 12. Possible structure for species C in Scheme I.

Hydrogen Activation Step. The mechanism discussed above satisfies the observed rate law and is consistent with the general spectral and kinetic observations on the system. The important question now arises as to the manner by which the reactive species C functions in the catalytic cycle, i.e., whether more than one Ru center is involved or, if activation occurs at only one Ru center, which center is favored. The reactive species C can be visualized as having the structure shown in Figure 12. The ruthenium atom Ru_a is coordinatively less saturated with respect to acetate compared to the other two ruthenium atoms Ru_b. Each of the ruthenium atoms b has an extra σ-donor acetate ligand. This may result in the delocalization of the electron density on the three ruthenium atoms such that Ru atom a becomes effectively an electron-richer center. This leads to the expectation that site Ru_a is probably a preferential center for the activation of either or both of the reactants. The reaction of species C with hydrogen in the absence of a reducible substrate showed a noticeable inhibition on the addition of protons which strongly suggests that the rate-determining step in the hydrogen-activation process by species C involves a heterolytic splitting of the hydrogen molecule with the release of a proton.[10] However, this result does not rule out the formation of a three-centered intermediate

I

which has a significant Ru···H interaction prior to the heterolytic splitting.[12] The fact that the rate of hydrogen reduction of species C is insensitive to the presence of added acetate salt[10] makes it uncertain whether the released proton in the hydrogen activation process is stabilized by an oxygen anion (i.e., the central oxygen of species C) or an acetate group. The independence of the rate on added acetate suggests, however, that if the stabilization of the proton produced in the heterolytic splitting is by an acetate group, the acetate is likely to be a bridging one. For if the nonbridging acetate is used,

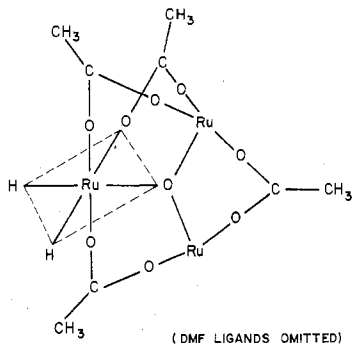

Figure 13. Possible structure for species D in Scheme I.

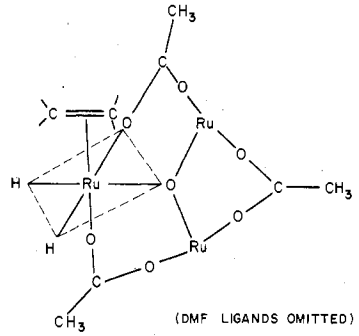

Figure 14. Possible structure for species E in Scheme I.

a rate enhancement for experiments performed with added acetate should be observed. Consequently, if a bridged acetate stabilizes the proton, a Ru_b center is most likely used for H_2 activation. However, if the O^{2-} group is the proton stabilizer, either Ru_a or Ru_b could be operating. In this case Ru_a may be more favorable sterically.

Although it is not clear, from the reaction in the absence of a substrate, which ruthenium atom is invoked in the activation process, the hydrogenation reaction provides information which favors one possibility over the other. The maximum rate of the hydrogenation of dec-1-ene was shown to be insensitive to the presence of added protons. This indicates that in the presence of substrate the release of a proton in the hydrogen activation step does not occur and the substrate interaction with I is a highly competitive process. In other words, the Ru···H formation in the activated complex is as significant as the H···H breaking. The interaction of the hydrogen molecule with species C is likely to delocalize the electron density toward the activating Ru center. Thus, a Ru^{III}_3 dihydride may be formed (i.e., species D in Scheme I). A possible structure for species D is shown in Figure 13.

The presence of an olefinic substrate prevents decomposition of species D via heterolytic splitting of the hydrogen. Furthermore, the inhibition of added acetate on the maximum rate of the hydrogenation of dec-1-ene requires a displacement of an acetate group by the substrate in a reversible rate-determining step (step 3 in Scheme I). This has two very significant implications: (i) *only one* Ru atom of species C is involved in activating both the hydrogen molecule and the substrate molecule; (ii) the Ru center involved is one of the b sites. If the Ru_a center or the Ru_b center which does not contain the bond H_2 were to bind the olefin, displacement of a bridging acetate by olefin would not be required as such centers contain solvent molecules which would be more labile than bridged ligands. Also consistent with the use of only one Ru_b atom in activating both the hydrogen molecule and the substrate molecule is the reactivity order observed for various octenes (Table I). These results can easily be rationalized by the importance of a steric effect which would result when both hydrogen and olefin are activated at the same Ru_b site. A

possible structure for the reactive intermediate (species E) is shown in Figure 14.

The average value obtained for the deuterium isotope effect (i.e., k_H/k_D) for the hydrogenation of dec-1-ene was 1.30. Such small isotope effects have been rationalized[15] in terms of metal–hydride bond formation and hydrogen–hydrogen bond breaking occurring in a concerted process. However, this is not inconsistent with the suggestion that a three-centered species (i.e., MH_2) such as species D in Scheme I is an intermediate,[12] which in the absence of a substrate gives rise to a heterolytic splitting of hydrogen in which case (k_H/k_D) observed had a value of 1.32.[10]

Hydride Transfer Step. No isomerization products were detected in the reaction mixture during the entire hydrogenation process. Also μ_3-oxo-triruthenium acetate was found to be reactive toward the hydrogenation of internal olefins. Consequently the nature of the hydride transfer step is uncertain as to whether it occurs in a stepwise or a concerted fashion and whether the addition is stereochemically cis or trans.

Experiments were carried out with DMF solutions of $[Ru_3O(OCOCH_3)_4(DMF)_n][OCOCH_3]$ in which maleic acid was used as the substrate and deuterium was used in place of hydrogen. The infrared spectra of the resultant deuterated succinic acid was thoroughly examined. Characterization of the different stereochemical forms of deuterated succinic acid via their infrared spectra has previously been reported.[16] The IR spectra of the resultant deuterated succinic acid from the deuteration of maleic acid showed strong bands at ca. 5.72 μ and at ca. 7.82 μ which are characteristic of DL symmetrically dideuterated succinic acid. The spectra also showed shoulders at ca. 7.9, 10.25, and 11.55 μ; this is indicative of the presence of meso symmetrically dideuterated succinic acid. The presence of the unsymmetrically dideuterated succinic acid was indicated by the presence of strong bands at ca. 8.1, 8.37, 8.65, and at 9.47 μ. The presence of the unsymmetrically dideuterated succinic acid provides good evidence for the stepwise addition of the hydrogen atoms to the unsaturated substrate.[17] On the transfer of the first hydrogen atom a σ-alkyl complex is formed which may exist in an equilibrium with the olefin dihydride complex as shown in reaction 14.

The presence of both the meso and the DL symmetrically dideuterated succinic acid does not provide conclusive evidence for the stereochemistry of addition, since an isomerization to

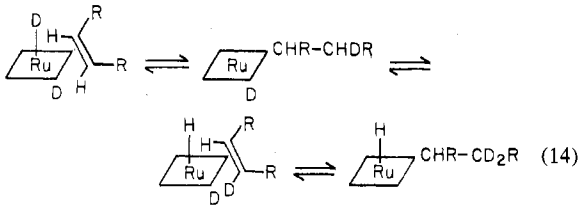

(14)

fumaric acid could be occurring. This does, however, confirm the stepwise addition of the hydrogen atoms.

Acknowledgment. The authors are grateful to the National Research Council of Canada for financial support of this research and to Engelhard Industries Ltd. for a loan of the ruthenium.

Registry No. Dec-1-ene, 872-05-9; oct-1-ene, 111-66-0; oct-2-ene, 111-67-1; cyclooctene, 931-88-4; hex-1-en-3-ol, 4798-44-1; cyclohex-2-en-1-ol, 822-67-3; cyclohex-3-en-1-ol, 822-66-2; hex-1-yne, 693-02-7; oct-1-yn-3-ol, 818-72-4; *trans*-stilbene, 103-30-0; maleic acid, 110-16-7; maleic anhydride, 108-31-6; diethyl maleate, 141-05-9; pentanone-3, 96-22-0; C_2H_4, 74-85-1; O_2, 7782-44-7; $[Ru_3O(OCOCH_3)_6(H_2O)_3][OCOCH_3]$, 38998-79-7; $[HRu_3O(OCOCH_3)_5(DMF)_3][OCOCH_3]$, 68024-44-2; $[Ru_3O(OCOCH_3)_6(DMF)_3][OCOCH_3]$, 68024-52-2; $LiOCOCH_3$, 546-89-4.

References and Notes

(1) B. Delmon and G. Jannes, *Catal. Proc. Int. Symp.*, 15–25 (1975).
(2) B. R. James, *Inorg. Chim. Acta Rev.*, **4**, 73 (1970).
(3) B. R. James, "Homogeneous Hydrogenation", Wiley, New York, N.Y., 1973, pp 72–103, 416–418.
(4) R. M. Laine, R. G. Rinker, and P. C. Ford, *J. Am. Chem. Soc.*, **99**, 252 (1977).
(5) A. Dobson and S. D. Robinson, *Platinum Met. Rev.*, **20**, 56 (1976), and references therein.
(6) R. M. Mitchell, A. Spencer, and G. Wilkinson, *J. Chem. Soc., Dalton Trans.*, 846 (1973).
(7) A. Spencer and G. Wilkinson, *J. Chem. Soc., Dalton Trans.*, 1570 (1972).
(8) P. Legzdins, R. W. Mitchell, G. L. Rempel, J. D. Ruddick, and G. Wilkinson, *J. Chem. Soc., A*, 3322 (1970).
(9) B. R. James and G. L. Rempel, *Can. J. Chem.*, **44**, 233 (1966).
(10) S. A. Fouda, B. C. Y. Hui, and G. L. Rempel, *Inorg. Chem.*, **17**, 3213 (1978).
(11) P. S. Hallman, B. R. McGarvey, and G. Wilkinson, *J. Chem. Soc. A*, 3143 (1968).
(12) B. C. Y. Hui, W. K. Teo, and G. L. Rempel, *Inorg. Chem.*, **12**, 757 (1973).
(13) S. A. Fouda and G. L. Rempel, unpublished results.
(14) F. R. Hartley, *Chem. Rev.*, **73**, 163 (1973).
(15) Reference 3, p 407.
(16) C. R. Childs, Jr., and K. Block, *J. Org. Chem.*, **26**, 1630 (1961).
(17) B. C. Y. Hui and B. R. James, *Can. J. Chem.*, **52**, 348 (1974).
(18) The fair linearity of the plot suggests that the variation in $[OCOCH_3^-]$ with variation in [olefin] is relatively small.